

## FEDSM-ICNMM2010-' \$%&\$

### FULLY COUPLED FLUID-STRUCTURE INTERACTION SIMULATIONS OF VOCAL FOLD VIBRATION

Lucy T. Zhang\*

Xingshi Wang

JEC 2049, Department of Mechanical, Aerospace and Nuclear Engineering  
Rensselaer Polytechnic Institute  
Troy, NY 12180  
Email: zhanglucy@rpi.edu

#### ABSTRACT

*The human vocal folds are modeled and simulated using a fully coupled fluid-structure interaction method. This numerical approach is efficient in simulating fluid and deformable structure interactions. The two domains are fully coupled using an interpolation scheme without expensive mesh updating or re-meshing. The method has been validated through rigorous convergence and accuracy tests. The response of the fluid affects the elastic structure deformation and vice versa. The goal of this study is to utilize this numerical tool to examine the entire fluid-structure system and predict the motion and vocal folds by providing constant inlet and outlet pressure. The input parameters and material properties, i.e. elastic and density of the vocal folds used in the model are physiological. In our numerical results, the glottal jet can be clearly identified; the corresponding pressure field distribution and velocity field are presented.*

#### INTRODUCTION

Human vocal folds have been under investigation for many years for their complexity in deformation and self-oscillatory nature. In this work, we intend to use a novel numerical technique to study and analyze this fluid-driven self-oscillation problem. A

fluid-structure interaction method, the Immersed finite element method (IFEM) [1], is used with a semi-implicit coupling technique to improve the interfacial solutions and convergence. The fluid domain and solid are defined on two sets of meshes independently and governed by their own governing equations. These two computational domain is coupled by the interpolation functions. [2–6]. Incompressible Navier-Stokes equations are considered as governing equation for the fluid domain,

$$\nabla \cdot \mathbf{v}^f = 0, \quad (1)$$

$$\rho^f (\mathbf{v}_{,t}^f + \mathbf{v}^f \cdot \nabla \mathbf{v}^f) = -\nabla p^f + \mu^f \nabla^2 \mathbf{v}^f + \mathbf{f}^{FSI,f}, \quad \text{in } \Omega \quad (2)$$

where  $\mathbf{v}^f$  is the velocity,  $p^f$  is the pressure,  $\mu^f$  is the viscosity of the fluid. Here,  $\mathbf{f}^{FSI,f}$  is the fluid-structure interaction force calculated by Eq. (3), and distributed on to the fluid domain by the interpolation function we choose [7].

$$\mathbf{f}^{FSI,s} = -(\rho^s - \rho^f) \ddot{\mathbf{u}}^s + \nabla \cdot \boldsymbol{\sigma}^s - \nabla \cdot \boldsymbol{\sigma}^f + (\rho^s - \rho^f) \mathbf{g} \quad \text{in } \Omega^s, \quad (3)$$

Here,  $\rho^s$  and  $\rho^f$  are the solid and fluid densities;  $\boldsymbol{\sigma}^s$  and  $\boldsymbol{\sigma}^f$  are the internal stress of solid and fluid, respectively;  $\mathbf{u}^s$  is the solid displacement and  $\mathbf{g}$  is the solid body force. The vocal folds

\*Address all correspondence to this author.

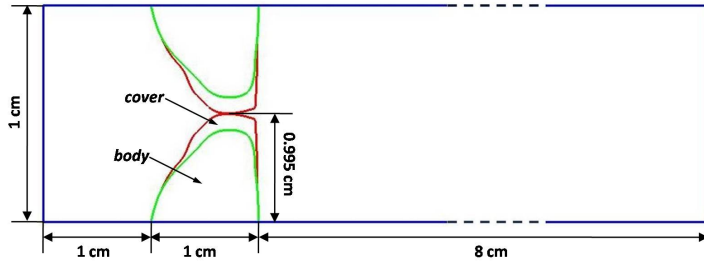


**FIGURE 1.** THE GEOMETRY OF 2-D COMPUTATIONAL DOMAIN.

are considered as hyperelastic materials with Mooney-Rivlin description [8]. Then the internal stress of the solid  $\sigma^s$  is determined by the solid strain and three material constants  $C_1$ ,  $C_2$ , and  $\kappa$ .

## GEOMETRICAL MODELS

The two-dimensional computational model of the vocal folds is shown in Fig. 1. The throat is assumed to be a 2-D channel with 2cm in width and 10cm in length. The vocal folds sit at 1cm from the entrance in the longitudinal direction. The geometry of the vocal fold is suggested by Tao [9]. To focus on the fluid domain and the interaction between the fluid and solid domain, only two layers, cover and body are considered in the vocal folds and the the ligament is included by the body. The two vocal folds are symmetric about the central line and with exact material descriptions. To avoid the upper and bottom vocal fold touching each other during the closing phase, a small value of glottal width,  $w_g = 0.001cm$  is set at the beginning. The opening of the vocal folds is driven by a pressure difference and the closing of the vocal folds is mainly governed by its intrinsic elastic property.

In this study, we take water as our working fluid, the body part is assumed to be twice stiffer than the cover parts of vocal folds. The throat channel is assumed to be no-slip steady wall and constant pressure difference  $\Delta p = 750dyn/cm^2$  is given between the inlet and outlet of the throat.

## RESULTS AND DISCUSSIONS

Based on our observation, we can divide our simulation results into two stages: Stage I from  $t = 0.4 \sim 0.6s$ , symmetric jet flow is generated at the glottis and the vortex dissipates and passes down to the downstream along the central line; Stage II from  $t = 1.1 \sim 1.3s$ , Coanda effect shows up, the jet flow is no longer symmetric and the fluid flow attaches to one of the vocal folds. In both stages, fluid field is at a quasi-steady state and found to be periodical near the glottis. Snapshots at two typical moments  $t = 0.5$  and  $t = 1.3$  are shown in Fig. 2

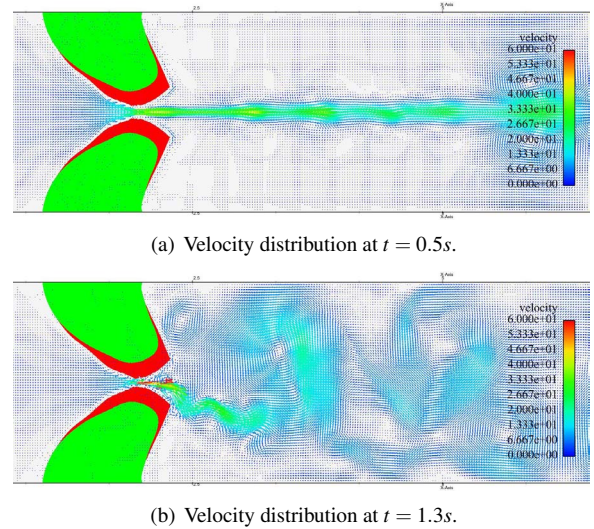


**FIGURE 2.** FLUID VELOCITY DISTRIBUTION.

To investigate the features of such self-oscillating fluid-structure interaction system, we will measure the time-history results of the following variables: 1) The glottis width  $w_g$  is defined as the minimum distance between the top and bottom vocal folds (labeled in Fig. 3), 2) the flow rate  $Q = \int v_x dy$  along vertical line  $B - C$  which is located at  $x = 1cm$  in the upstream of the folds, and 3) the velocity at the glottis with location  $x = 2cm, y = 1cm$  (marked as point  $A$  in Fig. 3).

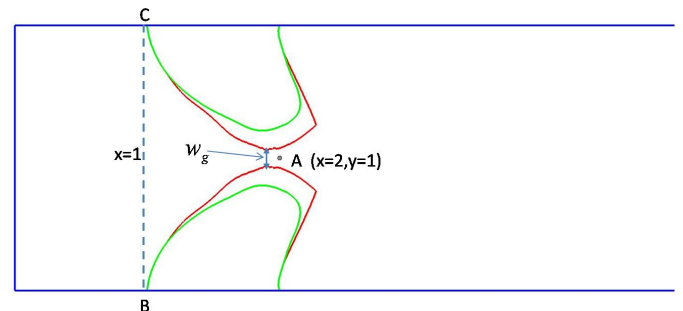
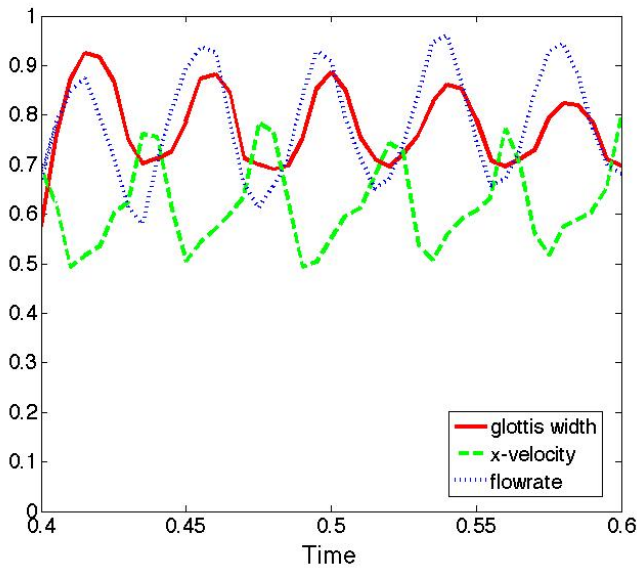


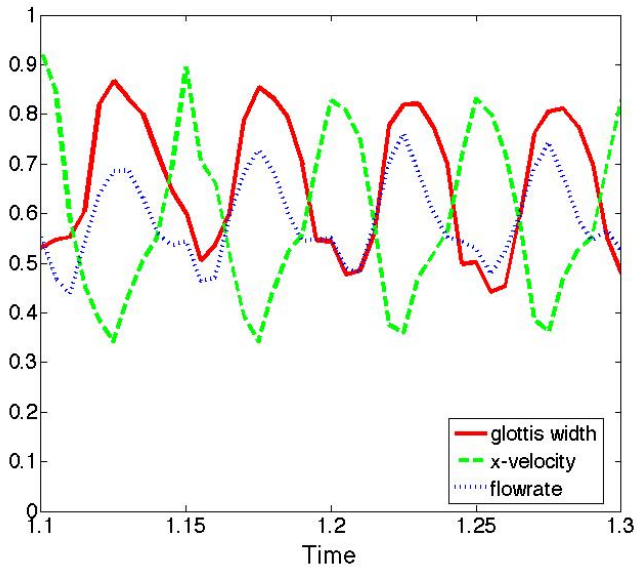
**FIGURE 3.** DEFINITION OF VARIABLES MEASURED.

The time history of these variables are plotted in Fig. 4. The results are separated into before and after the Coanda effect appears, i.e. Stage I and Stage II, respectively. All the variables here are normalized by their maximum values in time, which are found to be  $\hat{w}_g = 0.14cm$ ,  $\hat{v}_x = 60cm/s$  and  $\hat{Q} = 3.2cm^2/s$ , respectively.

Based on Figures 4, the periodical feature can be found in all four variables we measured during both Stage I and Stage



(a) Glottis width  $w_g$ , x component velocity  $v_x$  and flow rate  $Q$  during Stage I.



(b) Glottis width  $w_g$ , x component velocity  $v_x$  and flow rate  $Q$  during Stage II.

**FIGURE 4.** ALL THE VARIABLES ARE NORMALIZED BY THEIR MAXIMUM.

II. Comparing Stage I and Stage II, we find that although the mean values of  $w_g$ ,  $v_x$  and  $P_g$  do not change much, the variation seems to increase significantly during Stage II. However, the mean flow rate,  $Q$ , decreases from  $2.49\text{cm}^2/\text{s}$  to  $1.87\text{cm}^2/\text{s}$  going from Stage I to Stage II.

The pressure across the glottis ( $1 < x < 3\text{cm}$ ) at the center line is shown in Fig. 5 at different times throughout the simulation. It is again separated into the two stages for comparison. The large pressure drop across the glottis appears at  $x = 1.8 \sim 2.0\text{cm}$ . The maximum pressure drop occurs when the glottis width  $w_g$  reaches its minimum (Fig. 4). Decreasing pressure drop across the glottis happens when the glottis width increases. Accordingly, the minimum of the pressure drop corresponds to the maximum of glottis width. This result shows that the pressure difference between the upstream and downstream of the vocal folds is the driving force that pushes the vocal folds to open.

During Stage II with Coanda effect, we can find vortex in the supraglottal region as show in Fig. 2 and such vortex becomes stronger when the vocal folds open and very weak when the vocal folds close. The existence of the vortex in supraglottal region will provide additional resistance force for the vocal folds to open. However, it takes time for the vortex to build up and take effects, so there is a phase lag between the vocal folds vibration and the vortices as they try to push the vocal folds back. This is why with the Coanda effect, the minimum glottis width (at closed position) in Stage II is much smaller than in Stage I, while the maximum glottis width (at opened position) does not change much as shown in Fig 4.

## CONCLUSIONS

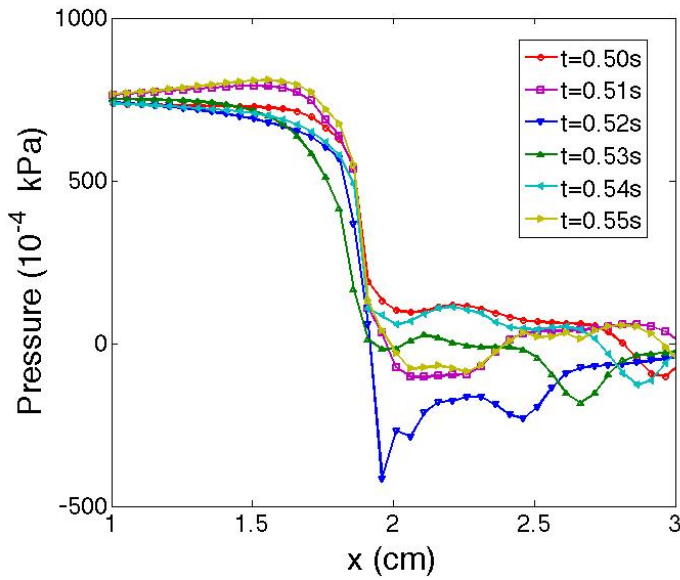
Immersed finite element method is used to simulate the vocal folds vibration problem. A symmetric glottal jet is captured from  $0.4\text{s}$  to  $0.6\text{s}$ . At approximately  $1.1\text{s}$ , with the growth of instability of the fluid field, the Coanda effect appears such that symmetric jet attaches to one side of the vocal fold randomly. The velocity and pressure fields of the fluid are significantly different before and after the Coanda effect. According, the vocal folds tend to vibrate at different states, with larger amplitude and smaller frequency after the Coanda effect shows up.

## ACKNOWLEDGMENT

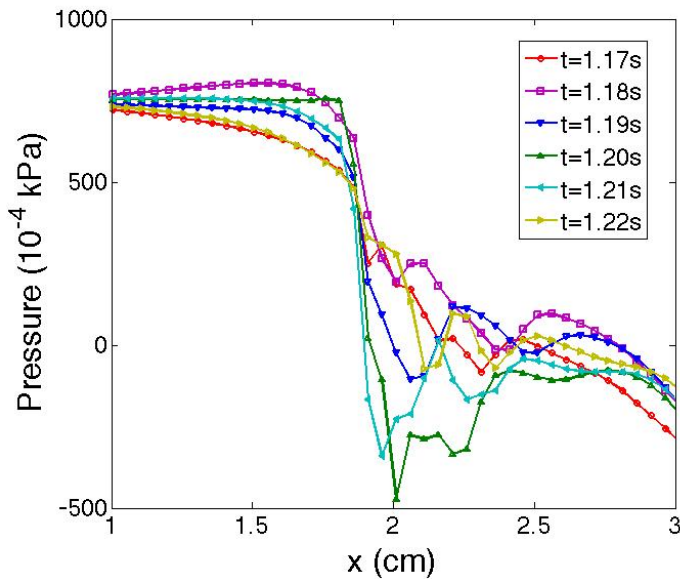
We would like to thank our collaborators Dr. Michael Krane and Dr. Timothy Wei for their comments and suggestions for this work.

## REFERENCES

- [1] Zhang, L., and Gay, M., 2007. "Immersed finite element method for fluid-structure interactions". *Journal of Fluids and Structures*, **23**, pp. 839–857.
- [2] Peskin, C., 2002. "The immersed boundary method". *Acta Numerica*, **11**, pp. 479–517.
- [3] Liu, W., Chen, Y., Chang, C., and Belytschko, T., 1996. "Advances in multiple scale kernel particle methods". *Computational Mechanics*, **18** (2), pp. 73–111.



(a) Pressure along the central line during Stage I.



(b) Pressure along the central line during Stage II.

**FIGURE 5.** PRESSURE ALONG THE CENTRAL LINE.

- [6] Li, S., and Liu, W., 1999. “Reproducing kernel hierarchical partition of unity. part I: Formulation and theory.”. *Computer Methods in Applied Mechanics and Engineering*, **145**, pp. 251–288.
- [7] Wang, X., and Zhang, L. T., 2010. “Interpolation functions in the immersed boundary and finite element methods”. *Computational Mechanics*, **45**, pp. 321–334.
- [8] Wang, X., and Liu, W., 2004. “Extended immersed boundary method using FEM and RKPM”. *Computer Methods in Applied Mechanics and Engineering*, **193**, pp. 1305–1321.
- [9] Tao, C., and Jiang, J. J., 2007. “Mechanical stress during phonation in a self-oscillating finite-element vocal fold model”. *Journal of Biomechanics*, **40**, pp. 2191–2198.

[4] Liu, W., and Chen, Y., 1995. “Wavelet and multiple scale reproducing kernel method”. *International Journal for Numerical Methods in Fluids*, **21**, pp. 901–932.

[5] Liu, W., Jun, S., and Zhang, Y., 1995. “Reproducing kernel particle methods”. *International Journal for Numerical Methods in Fluids*, **20**, pp. 1081–1106.